Research Article Vol. 58, No. 5 / 10 February 2019 / Applied Optics A251

applied optics

Holographic waveguide head-up display with 2-D pupil expansion and longitudinal image magnification

Craig T. Draper,[1,*] Colton M. Bigler,[1] Micah S. Mann,[1] Kalluri Sarma,[2] and Pierre-Alexandre Blanche[1,3]

[1]College of Optical Sciences, University of Arizona, 1630 E. University Blvd., Tucson, Arizona 85721, USA
[2]Honeywell, Advanced Technology, 21111 N. 19th Avenue, M/S 2J35, Phoenix, Arizona 85027, USA
[3]e-mail: pablanche@optics.arizona.edu
*Corresponding author: cdraper1@email.arizona.edu

Received 14 September 2018; revised 20 December 2018; accepted 26 December 2018; posted 2 January 2019 (Doc. ID 345913); published 4 February 2019

Head-up displays (HUDs) are used in aircraft to overlay relevant flight information on the vehicle's externals for pilots to view with continued focus on the far field. In these systems, the field of view (FOV) is traditionally limited by the size of the projection optics. Though classical HUD systems take a significant amount of space in the flight deck, they have become a necessity in avionic transportation. Our research aims to reduce the size of the HUD footprint while offering a wide FOV projected in the far field with an expanded pupil. This has been accomplished by coupling the image-bearing light into a waveguide under total internal reflection conditions, redirecting that light in the orthogonal direction, and then outcoupling the light toward the pilot. Each step was achieved using holographic optical elements. The injection hologram has optical power to obtain longitudinal magnification, whereas the redirection hologram expands the pupil in one dimension and the extraction hologram expands the pupil in a second dimension. Varying diffraction efficiency along the direction of the light propagation ensures even image intensity throughout the expanded pupil. We used ray tracing optical simulations to optimize the design of the system and present a fully operational demonstrator of the HUD. This HUD produces an image with a FOV of 24° × 12.6° at a viewing distance of 4.5 in. (114 mm) from the waveguide, with infinite longitudinal magnification and 1.9× by 1.6× horizontal and vertical pupil expansion, respectively.

https://doi.org/10.1364/AO.58.00A251

1. INTRODUCTION

Head-up displays (HUDs) are being deployed in transportation vehicles such as automobiles and aircraft to reduce the amount of time spent looking away from either the road or sky in comparison to a head-down display. This advantage helps improve the pilot situational awareness and reduces reaction time [1–5]. There exist many versions of HUDs, the simplest of which consist of using a smartphone sitting on a dashboard with the image reflected by the windshield into the driver's eyes. Unfortunately, this version does not provide the image at the same focal distance as the road, forcing the eye to accommodate. The current avionics HUD uses a combiner, with a dichroic mirror or a hologram, to reflect a collimated image into the user's eyes. This method effectively superimposes an image onto the far field by using a system of lenses to expand and collimate an image from the projector, as seen in Fig. 1 [6,7].

The limitations of the traditional airliner HUD stem from the footprint of the system where the field of view (FOV) or perceived image depends on the size of the projection optics. In areas such as an avionics cockpit or automobile dashboard, space is severely restricted forcing an ultimate limit on FOV achievable. Another issue is the narrow area where an operator can view the entire projected image. This area is called the eye box and is determined by the triangle formed by the image (located at infinity), the surface of the combiner, and the viewer location presented in Fig. 1. Accordingly, the larger the combiner, the larger the eye box and FOV can potentially be.

These limitations on the footprint of the system, eye box size, and FOV in traditional HUDs have researchers looking for other solutions, such as freeform optics, multi-mirror elements, and waveguides [8–11]. Here, we present an original HUD configuration with a small footprint that uses holographic optical elements (HOEs) in combination with waveguide optics to

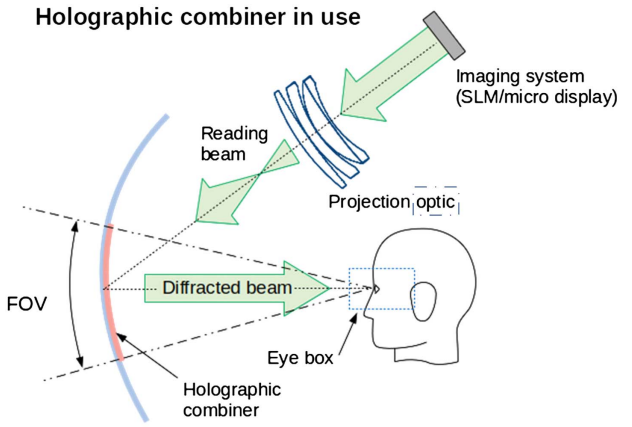

Fig. 1. Traditional aircraft HUD with holographic combiner for image projection.

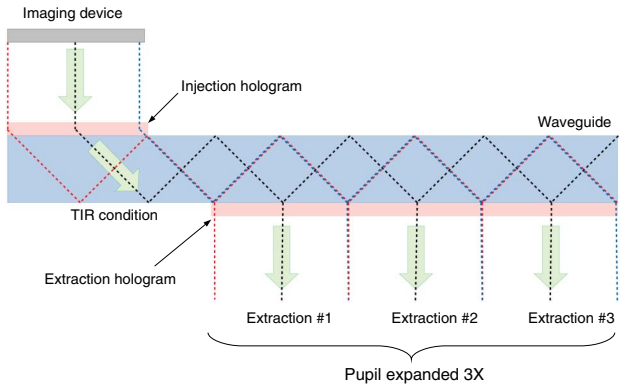

Fig. 3. Schematic showing one-dimensional pupil expansion where an image is recirculated and extracted multiple times.

increase both the eye box and the FOV while keeping the image projected at infinity.

Figure 2 shows the configuration of the HUD system we pursued, where three edge-lit HOEs on a waveguide effectively reduced the HUD size while still offering a wide FOV over a large area. This is accomplished by inserting an image into the waveguide using an injection hologram that has optical power to collimate and diffract the image. The diffraction angle is such that the light is coupled inside the waveguide by total internal reflection (TIR) and propagates horizontally along the length of the waveguide.

The light is then redirected vertically along the length of the waveguide with a second hologram while keeping the TIR condition. The diffraction efficiency of the redirection hologram is less than a 100% so the light that is not redirected continues its travel inside the waveguide and is only redirected after further interaction with the hologram.

The light that is now propagating vertically is then diffracted toward the viewer thanks to an extraction hologram. The light that is not diffracted after the first interaction with this hologram continues its travel inside the waveguide in the vertical direction and is eventually extracted after further interaction with the hologram. The efficiency profile of the redirection and extraction holograms will be discussed in Section 2.B.

By recirculating the light several times within the waveguide, the redirection and extraction holograms expand the pupil in the horizontal and vertical directions, respectively. It is to be noted that this pupil expansion does not change the image magnification, which is only due to the optical power of the injection hologram. Also, since the image is focused at infinity, multiple extractions do not replicate the image but expand the eye box. From the viewer perspective, the HUD system presents a single, collimated, magnified image across an expanded eye box.

Figure 3 shows the process of pupil expansion in one dimension where an image is coupled into a waveguide beyond TIR conditions and splits along the extraction hologram to achieve multiple extractions of the same image.

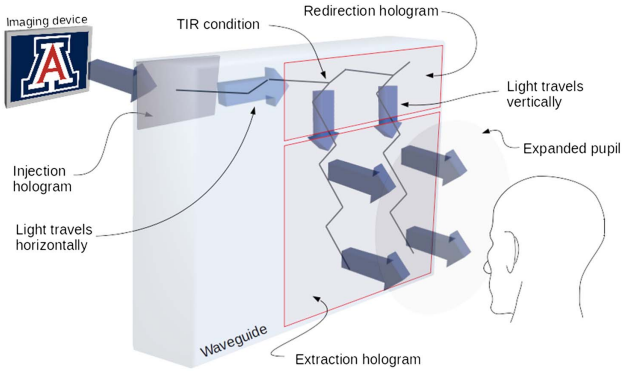

Fig. 2. Conceptual design of the HUD system showing the different hologram sections that couple the image inside the waveguide, redirect it internally, and extract the light with two-dimensional pupil expansion for an increased eye box.

2. HOLOGRAM DESIGN

Our HUD system consists of three edge-illuminated holograms labeled the injection, the redirection, and the extraction. The holograms are applied onto a planar waveguide surface. The specifics of each hologram are as follows.

A. Injection Hologram

The injection hologram is designed such that it has optical power and redirects the image inside the waveguide at TIR. The hologram collimates an expanding beam located in front of the waveguide surface and redirects it within the waveguide. This angle allows the diffracted beam to propagate internally without overlap or gaps between reflections concerning the size of the hologram and waveguide thickness. Encoding optical power into the injection hologram removes the need for optics to magnify the image and optics to locate it at infinity.

B. Redirection Hologram

The redirection hologram was designed to receive the collimated beam propagating horizontally inside the waveguide and diffract it in the vertical direction. The angle allows propagation without overlap or gaps between the different TIR bounces, which would result in dark areas in the projected image.

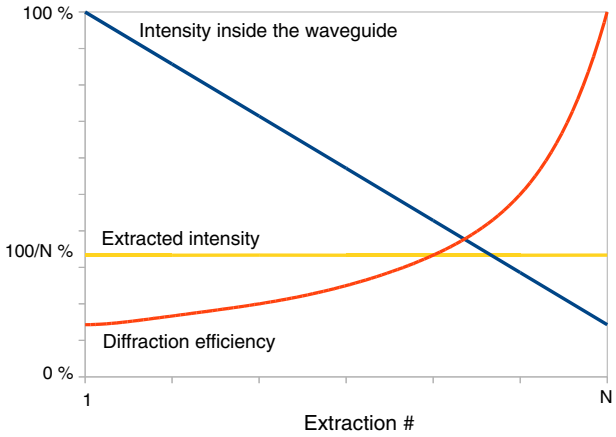

Fig. 4. Longitudinal diffraction efficiency profile (red) of the redirection and extraction holograms according to the number of interactions with the hologram to compensate for the reduction of intensity inside the waveguide (blue) to keep the extracted intensity constant (yellow).

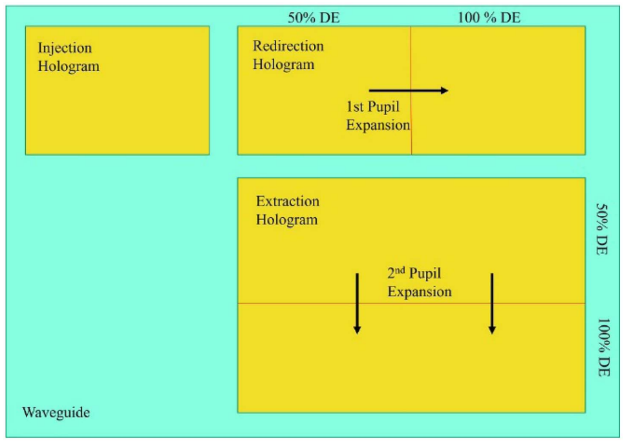

Fig. 5. Schematic of the HUD systems showing the three sections of holograms with modulated DE values to achieve pupil expansion in two dimensions.

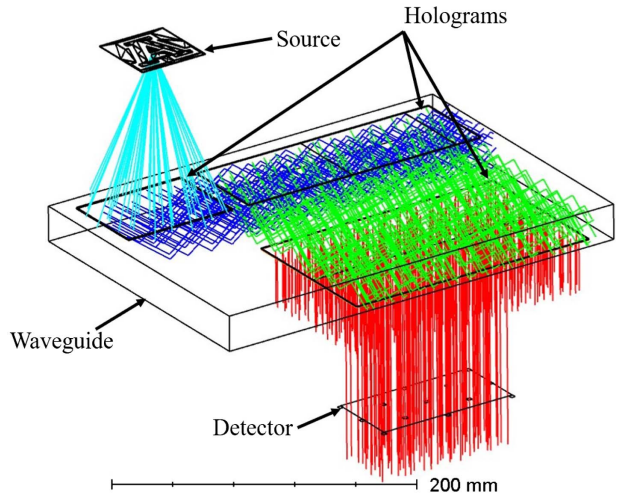

Fig. 6. Isometric view of our Zemax model showing point source reading beam propagating through the system and extracted normal to the waveguide surface. A color code was assigned to show each section the image undertakes: cyan, source to injection hologram; blue, injection hologram to redirection hologram; green, redirection hologram to extraction hologram; red, extracted light to detector.

The pupil is expanded laterally by the multiple diffractions of the image across the length of the hologram. To ensure a uniform image intensity through the entire pupil, the diffraction efficiency (DE) varies across the width of the hologram. Each time the light interacts with the hologram, some portion is diffracted, which leaves less intensity inside the waveguide to be diffracted by the subsequent interactions.

If I_0 is the initial intensity injected inside the waveguide, and N is the number of extractions, the maximum uniform image intensity is given by I_0/N. The residual light propagating inside the waveguide after the first interaction is $I_0 - I_0/N$. After the second interaction this intensity is $I_0 - 2I_0/N$, and after the nth interaction it is $I(n) = I_0[1 - (n-1)/N]$. To have constant intensity diffracted by the hologram while the incident intensity $I(n)$ decreases, the DE of the different sections of the hologram should increase such that $\mathrm{DE}(n) * I(n) = I_0/N$ or $\mathrm{DE}(n) = 1/(N - n + 1)$.

Figure 4 shows the diffraction efficiency profile (red) required to compensate for the decreased intensity remaining in the waveguide (blue) to keep the diffracted light constant (yellow).

C. Extraction Hologram

The extraction hologram was designed to receive the collimated beam from the redirection hologram and diffract the collimated beam toward the user. By outcoupling a collimated beam the image is located at infinity. The pupil was expanded by multiple extractions, and the uniformity of the extracted image intensity was guaranteed by varying diffraction efficiency across the hologram, as explained earlier in Section 2.B.

3. COMPUTER SIMULATION

The holographic waveguide HUD design was optimized using the optical simulation software Zemax Optic Studio and a coupled-wave analysis program to calculate the angular and spectral dispersion of the holograms. Figure 5 shows the configuration and Fig. 6 shows a ray tracing of the HUD where a point source is collimated, propagates throughout the waveguide, and is extracted toward an array of detectors.

A BK7 300 by 200 by 25.4 mm slab of glass was used as the waveguide with an index of refraction of 1.5195 at a wavelength of 532 nm.

The hologram lens feature was used in Zemax to simulate the HOE's function. The 60 by 80 mm injection hologram, with a focal length of 114 mm, redirects the beam as an edge-lit hologram to satisfy TIR conditions at 60°. 10 mm from the injection hologram, the redirection hologram at 60 by 180 mm was placed as a reflection hologram with three sections of varying reflectivity, which simulated the varying diffraction efficiency. Its recording geometry allows incident light from the injection hologram to be diffracted 90° at an angle of 52° to

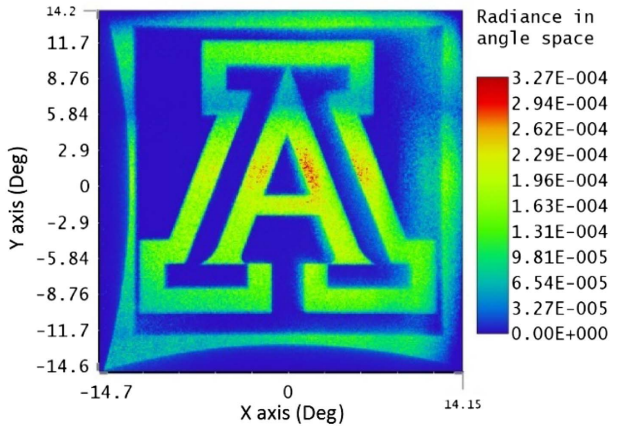

Fig. 7. Angular radiance of Zemax detector 114 mm behind extraction hologram on BK7 waveguide showing perceived image at infinity occupying a maximum FOV of 28° by 28°.

satisfy TIR conditions. 10 mm from the redirection hologram, the extraction hologram at 110 by 180 mm consists of two sections where one reflects 50% of the light while diffracting the other 50%, and the other section has a 100% efficiency diffracting all the remaining incident light.

The extracted light is directed toward an array of human eye pupil-sized detectors (3 by 3 mm) spread across a 50 by 100 mm eye box, 114 mm away from the waveguide. These parameters yielded an expanded eye box with a FOV of 28° by 28°, as seen in Fig. 7.

The FOV depends on the distribution of angles that can propagate throughout the waveguide. Since the minimum angle is the critical angle, materials with a higher refractive index allow for a larger FOV. It was found that to achieve a 40° by 40° FOV, a refractive index of at least 1.8 should be used for the waveguide. However, these specialty glasses come at a higher cost and were unavailable for the recording of the demonstrator.

The Kogelnik coupled-wave analysis [12] was used to supplement the Zemax model regarding the angular selectivity of the HOEs. This analysis showed that the diffraction efficiencies of the edge-lit injection and redirection holograms have a limited acceptance angle for a monochromatic source. At the design wavelength of 532 nm, the full width half-maximum system efficiency is only 0.5°. By using a polychromatic source, the angular selectivity of the hologram can be increased thanks to the superblaze (envelope of all the dispersion curves at various wavelengths) characteristic of the holograms, shown in blue in Fig. 8. This demonstrates that the HUD would require a polychromatic image source to achieve a larger FOV.

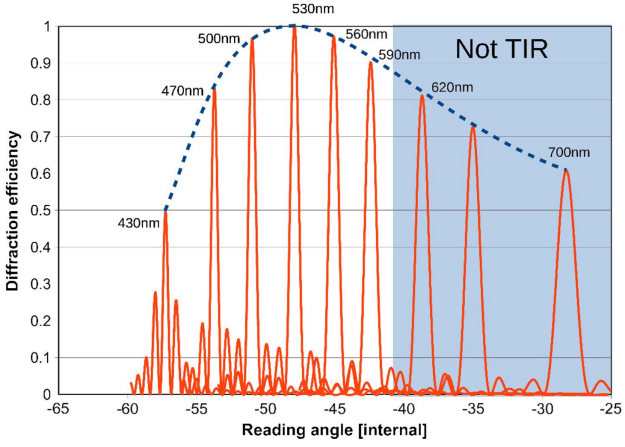

Fig. 8. Diffraction efficiency computation according to both incident angle in degrees and wavelength for the redirection hologram geometry, using the Bayfol HX200 material parameters (16 μm thickness). Angles shallower than 41.8° are not under TIR conditions.

4. PROOF OF CONCEPT DEMONSTRATOR

A demonstrator was created after optimizing the system configuration using the optical simulation software Zemax and the coupled-wave analysis.

The waveguide was made of Saint Gobain Diamant glass, which is a low iron, highly transparent material with very little residual color compared to the more traditional soda—lime—silica float glass. The Diamant glass replaced BK7 from the simulation due to its exceptional optical transmission properties and similar refractive index experimentally determined to be 1.52. All the holograms were recorded using the Covestro Bayfol HX200 photopolymer.

A. Hologram Recording

The holograms were recorded from the interference of a doubled Nd YAG laser at 532 nm split into a reference and object beam. Using 18 mJ/cm^2 exposure dosage and a polarization orthogonal to the Bragg planes being recorded gave a maximum of 96.7% DE. The recording polarization affects the max DE obtainable [13]. Prism couplers were used to insert the beams at TIR inside the waveguide. Index matching was ensured using microscope objective immersion oil. We chose to make the injection hologram 65 by 85 mm, redirection 65 by 160 mm, and extraction hologram 105 by 160 mm all spaced 10 mm apart in reflection geometry.

A polarization rotation was noticed in the diffracted light from the injection hologram. Because of the sensitivity to polarization during the recording of the hologram, it was not possible to directly use the light diffracted by the injection hologram to record the redirection and extraction holograms. Instead, we record each hologram independently from each other, having neither object or reference beams passing through earlier holograms.

To achieve a compact system and increase the image magnification capability, the injection hologram should have the shortest focal length possible. To do so, we used the light expanded by a microscope objective (60×) as the object beam, while the reference beam is collimated and incident at 60°. Using this configuration, the object plane of the system is located at the focus of the microscope objective.

To achieve the modulated DE required for the redirection and extraction pupil expansions, as discussed in Section 2.B, the material was pre-exposed. The pre-exposure method starts the polymerization process in the photopolymer, effectively reducing the maximum DE capacity. The pre-exposure is done by illuminating the material with a single homogeneous beam before recording the interference pattern with both reference

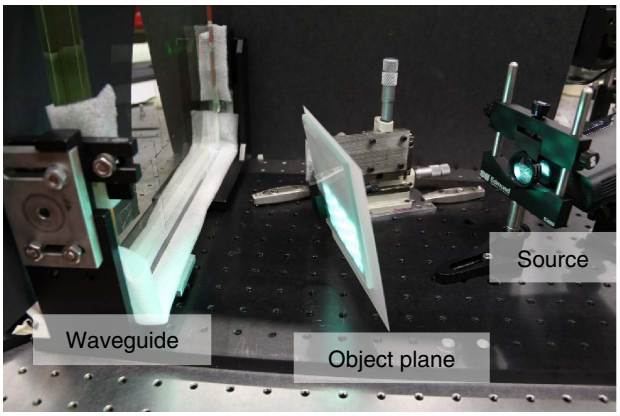

Fig. 9. Object plane of the HUD showing the required tip and tilt with respect to waveguide surface to compensate for polychromatic dispersion.

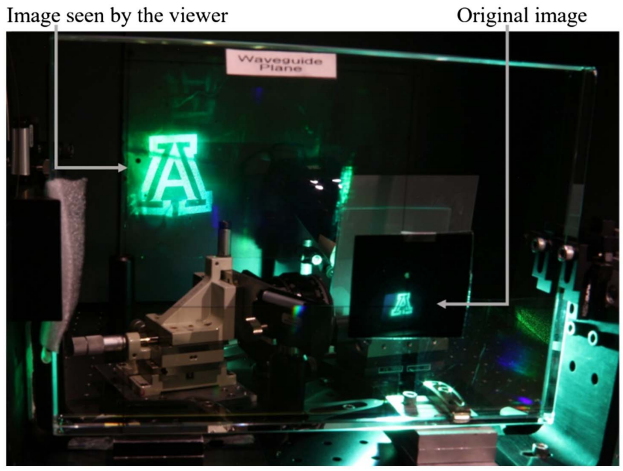

Fig. 11. Picture of the prototype HUD system using a high f-number camera objective resulting in large depth of view for object and image planes in focus. Notice the small injection image that is magnified as the outcoupled image.

and object beams at normal recording power. A 5.5 mJ/cm^2 pre-exposure at 532 nm was found to reliably yield 50% DE.

B. System Testing

We used a pico projector as a polychromatic light source for the HUD. However, due to the spectral selectivity of the holograms only the green portion of the spectrum, centered on 532 nm, is efficiently transmitted through the system. Nonetheless, the dispersion allows wavelengths of ±20 nm to propagate at different angles, with the smaller angles being redshifted (532 + 20 nm) and larger angles being blueshifted (532–20 nm).

This spectral shift has an important implication on the geometry of the object plane. The focal distance of a diffraction lens depends on the wavelength, being shorter for larger wavelengths. If the object plane is strictly parallel to the waveguide, the blueshifted and redshifted parts of the image are out of focus and do not overlap correctly with the central green image, yielding image distortion and splitting. To compensate for this effect, the object plane was tilted 7° in the vertical direction and 15° in the horizontal direction, as seen in Fig. 9. These values were found experimentally.

The spatial resolution of the HUD was observed using a standard U.S. Airforce 1951 Test Target. The target was placed at the object plane and illuminated with a polychromatic source. The extracted image has a maximum insertion resolution of 12.7 lines per millimeter in the central field as it could be observed from Fig. 10. Image blurriness along the periphery is attributed to secondary aberrations, such as the need for a nonplanar object plane, and the flatness of the holographic material.

Figure 11 shows the respective size of the injected image (right) and the extracted image (left) demonstrating the image magnification by the system. As seen, a small projected source is magnified decreasing the required projector size from traditional HUD systems.

Figures 12 and 13 show pictures of the HUD taken with a DSLR camera with a background image of a runway located in the far field. Figure 12 was taken with the camera focused on the waveguide plane, showing that both the far-field image and

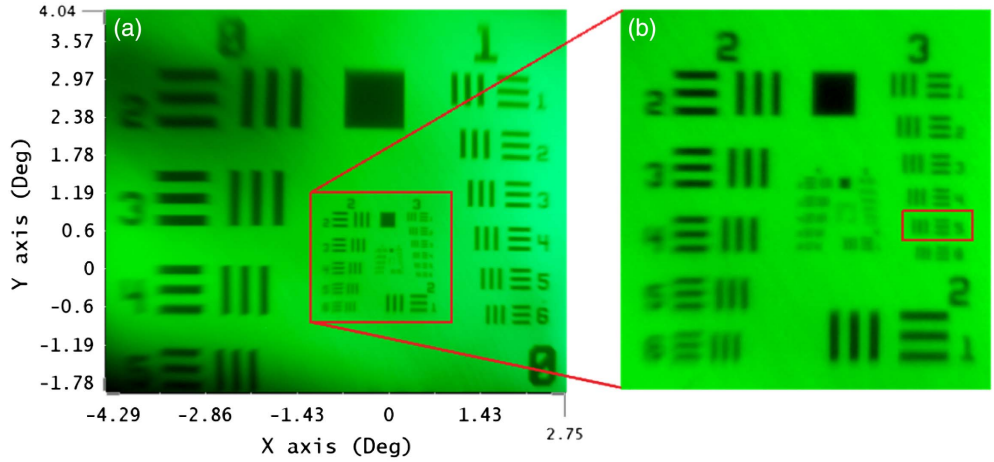

Fig. 10. Image of a U.S. Air Force Resolution Target through the HUD showing a resolution of 12.7 lp/mm in the central field of view. (a) is outcoupled image while (b) is enlarged.

Fig. 12. Picture of the HUD system taken with a DSLR camera when focused at the location of the waveguide. The background runway is displayed on a monitor located in the far field; the symbology (green) is projected at infinity through the HUD system.

Fig. 13. Picture of the HUD system taken with a DSLR camera when focused at infinity. The background runway is displayed on a monitor located in the far field; the symbology (green) is projected at infinity through the HUD system.

the symbology projected through the HUD system are out of focus. In Fig. 13, the camera is focused at infinity and the symbology projected by the HUD overlays the image located in the far field. This demonstrates that the user does not have to accommodate to see the image.

The FOV was determined by imaging the output light from the extraction hologram with a lens and measuring the size of the image relative to the focal length. A monochromatic light source produced a FOV of only 8.1° by 6.6° due to the angular selectivity of the holograms, as discussed in Section 3. However, using a polychromatic source, the FOV is extended to 24.1° by 12.6°, in the horizontal and vertical directions, respectively.

5. CONCLUSION AND FUTURE WORK

A HUD using HOEs on a waveguide can effectively offer a solution to the size limitations of traditional HUDs. Our prototype demonstrates a 24° by 12.6° FOV in the horizontal and vertical directions, respectively, over an 80 by 110 mm eye box with a max insertion resolution of 12.7 lines/mm. The expanded eye box was due to the 1.9× by 1.6× horizontal and vertical pupil expansion, respectively. Image magnification and image projection in the far field are a result of the injection hologram's optical power. HOEs had to be recorded individually due to polarization rotation effects in the diffracted light of edge-lit holograms. The chromatic dispersion requires a tilted object plane to ensure the correct focal distance. The prototype still shows some aberration in the projected image, especially in the peripheral field of view. The simulation does not reproduce these aberrations, leading us to believe that they are due to the imperfections of the hologram and the object plane. The object plane may be a curved asphere according to the focal length shift calculated from Bragg's law of diffraction.

The difference between the simulated FOV of 28° by 28° in Zemax and experimental FOV of 24° by 12.6° is due to Zemax's ability to calculate diffractive optics properties. It does not account for diffraction efficiency according to angular acceptance or wavelength acceptance. Zemax provided a geometrical limit on what will propagate through the system. Kogelnik coupled-wave analysis showed that each hologram has varying diffraction efficiency according to both angular and wavelength acceptance. The summation of the DEs results in a fall off along the edges yielding low image brightness along the edges and ultimately FOV limitation in the demonstrator.

It is possible to achieve an even larger FOV by using several monochromatic HOEs. In this case, multiple injection holograms (eventually multiplexed) will be overlaid on top of each other to inject the image at several angles. Rather than inject different colors, the multiplex holograms will inject multiple angles. This will increase the diffraction efficiency of the system by increasing the acceptance angle range for the HOEs.

Another option to increase the FOV is to use a higher refractive index waveguide, as seen in simulation. Using a dense flint glass, such as SF6 glass from Schott, would have a smaller critical angle increasing the range of angles that can propagate within the waveguide effectively increasing the FOV possible.

Full-color imaging can be achieved by having HOEs with red, green, and blue design wavelengths. This demonstrator had HOEs with only a green design wavelength. By having the primary colors of red, green, and blue, all colors can be created through color addition. These HOEs can also be multiplexed inside a single sheet of material. The tilt angles of the object plane of 7° and 15° will be similar. However, due to the nonlinearity of Bragg's law of diffraction in calculating focal point shift, chromatic aberration may be present toward the edges of the image.

The demonstrator we presented uses a parallel, planar waveguide for unaberrated image propagation. However, it should be possible to use a curved waveguide, as long as the radius of curvature is the same for the top and bottom surfaces. The hologram can be recorded to compensate for any residual optical power. The use of a curved waveguide could be interesting for a better integration of the HUD into confined environments, such as cars and small aircrafts.

Funding. Honeywell International Inc. (6400282571, 6400327460, 6400368337); National Science Foundation

(NSF) Arizona TRIF program and REU IOU-NA program (EEC-0812072, EEC-1659510, IIP-1640329); Technology Research Initiative Funding; Western Alliance to Expand Student Opportunities (f18ur041/f2018ur0052).

REFERENCES

1. Y.-C. Liu and M.-H. Wen, "Comparison of head-up display (HUD) vs. head-down display (HDD): driving performance of commercial vehicle operators in Taiwan," Int. J. Hum. Comput. Stud. **61**, 679–697 (2004).
2. M. AblaBmeier, T. Poitschke, F. W. K. Bengler, and G. Rigoll, "Eye gaze studies comparing head-up and head-down displays in vehicles," in *IEEE International Conference on Multimedia and Expo* (2007), pp. 2250–2252.
3. C. Wickens and P. Ververs, "Allocation of attention with head-up displays," Tech. Rep. DOT/FAA/AM-98/28 (Aviation Research Laboratory, Institute of Aviation, 1998).
4. S. Fadden, C. D. Wickens, and P. Ververs, "Costs and benefits of head up displays: an attention perspective and a meta analysis," SAE Technical Paper 2000-01-5542 (SAE International, 2000).
5. W. J. Horrey, C. D. Wickens, and A. L. Alexander, "The effects of head-up display clutter and in-vehicle display separation on concurrent driving performance," Proc. Hum. Factors Ergon. Soc. Annu. Meet. **47**, 1880–1884 (2003).
6. P. Coni, S. Hourlier, A. Gueguen, X. Servantie, and L. Laluque, "50–3: a full windshield head-up display using simulated collimation," SID Symp. Dig. Tech. Pap. **47**, 684–687 (2016).
7. P. Coni, S. Hourlier, X. Servantie, L. Laluque, and A. Gueguen, "A 3D head up display with simulated collimation," SAE Technical Paper 2016-01-1978 (SAE International, 2016).
8. J. Han, J. Liu, X. Yao, and Y. Wang, "Portable waveguide display system with a large field of view by integrating freeform elements and volume holograms," Opt. Express **23**, 3534–3549 (2015).
9. M. Homan, "The use of optical waveguides in head up display (HUD) applications," Proc. SPIE **8736**, 87360E (2013).
10. L. Gu, D. Cheng, W. Hou, and Y. Wang, "Design of two-dimensional waveguide head-up display," Proc. SPIE **10693**, 106930G (2018).
11. C. Bigler and P.-A. Blanche, and K. Sarma, "Holographic waveguide heads-up display for longitudinal image magnification and pupil expansion," Appl. Opt. **57**, 2007–2013 (2018).
12. H. Kogelnik, "Coupled wave theory for thick hologram gratings," Bell Syst. Tech. J. **48**, 2909–2947 (1969).
13. A. Scharmann and J. Ziller, "Influence of light polarization on the diffraction efficiency of TIR holograms," Opt. Commun. **24**, 181–184 (1978).